

Incorporation and Remodeling of Structural Allografts in Acetabular Reconstruction

Multiscale, Micro-Morphological Analysis of 13 Pelvic Explants

Sebastian Butscheidt, MD, Menard Moritz, MD, Thorsten Gehrke, MD, Klaus Püschel, MD, Michael Amling, MD, Michael Hahn, PhD, and Tim Rolvien, MD

Investigation performed at the Departments of Osteology and Biomechanics, Legal Medicine, and Orthopaedic Surgery, University Medical Center Hamburg-Eppendorf, and the Helios Endo Clinic Hamburg, Hamburg Germany

Background: Total hip arthroplasty (THA) is frequently accompanied by acetabular bone loss, which constitutes a major challenge in revision procedures. Structural allografts can be implanted to restore a stable osseous foundation for the acetabular prosthesis. As previous studies were limited to clinical data or included very few cases, the extent to which the graft bone is incorporated over time has remained unclear.

Methods: Thirteen acetabula were retrieved post mortem, and the incorporation properties of the bone allografts were analyzed using a hierarchical approach of imaging techniques including contact radiography, high-resolution peripheral quantitative computed tomography (HR-pQCT), histological analysis of undecalcified specimens, and quantitative back-scattered electron imaging (qBEI). The distance between the current allograft bone and host bone borders (i.e., current overlap) as well as the distance between the original allograft bone and host bone borders (i.e., total ingrowth) were assessed.

Results: In 10 of 13 cases, the complete interface (100%) was characterized by direct contact and additional overlap of the allograft bone and host bone, while the remaining 3 cases demonstrated direct contact along 25% to 80% of the interface. The allograft bone showed an intact trabecular structure and significantly higher mineralization compared with the host bone. The mean current overlap (and standard deviation) was 2.3 ± 1.0 mm, with a maximum of 5.3 ± 2.4 mm. Importantly, the total ingrowth reached much further, to a mean of 7.2 ± 2.3 mm (maximum, 10.5 ± 4.0 mm). Neither the time that the allograft was in situ nor the degree of contact between the host and allograft bone correlated with the current overlap and the time in situ did not correlate with total ingrowth.

Conclusions: This study showed bone remodeling with subsequent interconnection of the host and allograft bone along the majority of the interface, leading to adequate incorporation of the allograft. The lack of complete incorporation of the graft did not lead to graft collapse up to 22 years after revision surgery.

Clinical Relevance: Our study provides the first systematic multiscale evaluation of successfully implanted structural allografts and forms the scientific basis for their clinical use in revision THA.

A septic acetabular component loosening is one of the most common reasons for revisions of total hip arthroplasty (THA), accounting for 19.7% of such revisions¹, and is associated with bone loss of variable severity. These bone defects need to be considered in revision procedures, as a tight junction with only minimal movement between the implant and host bone is required for successful

osseointegration, which is essential for a functional and stable long-term outcome of arthroplasty². Reconstructive options include impaction grafting using cancellous chips and structural bone allografts^{3,4} as well as particulate bone⁵.

Bone allografts are the second most common “transplant” in humans after blood components⁶. Histological studies involving animals and humans have shown complete incorporation of

Disclosure: There was no outside source of funding for this study. The **Disclosure of Potential Conflicts of Interest** forms are provided with the online version of the article (<http://links.lww.com/JBJS/E854>).

Copyright © 2018 The Authors. Published by The Journal of Bone and Joint Surgery, Incorporated. All rights reserved. This is an open-access article distributed under the terms of the [Creative Commons Attribution-Non Commercial-No Derivatives License 4.0](https://creativecommons.org/licenses/by-nc-nd/4.0/) (CCBY-NC-ND), where it is permissible to download and share the work provided it is properly cited. The work cannot be changed in any way or used commercially without permission from the journal.

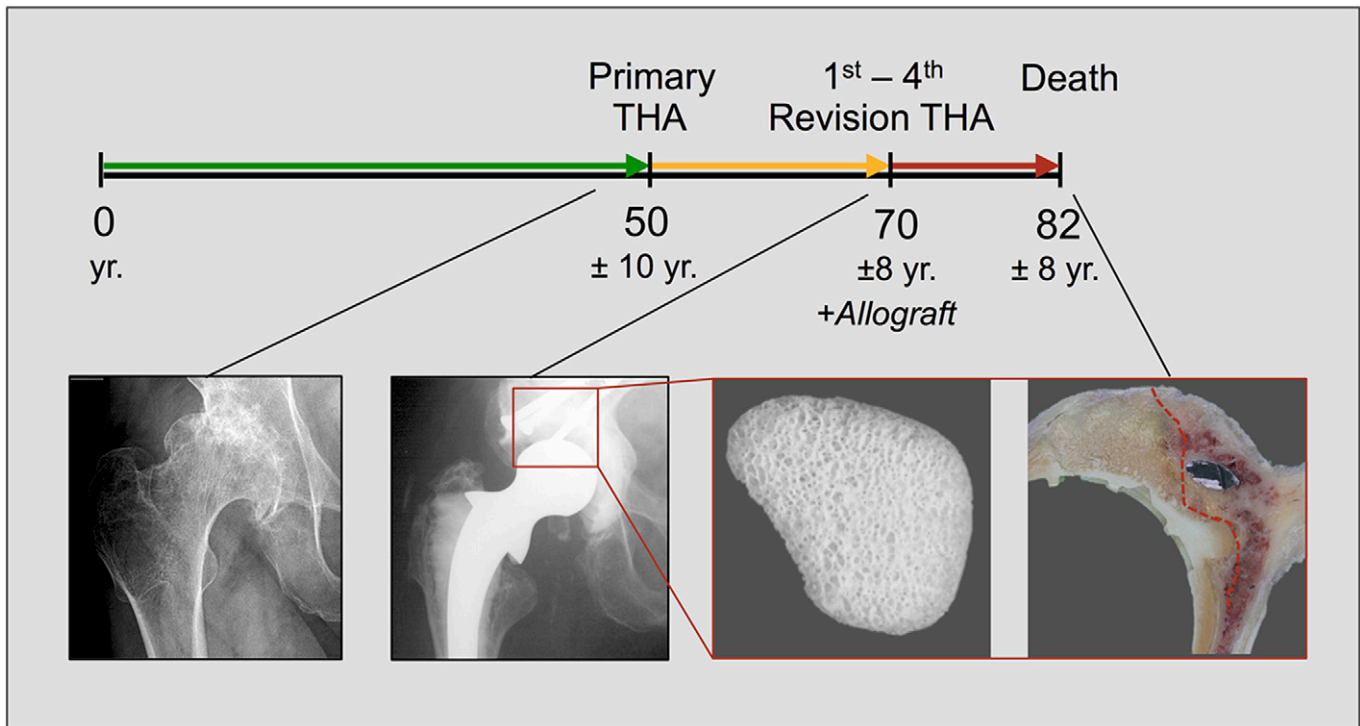


Fig. 1
Timeline demonstrating the ages at the primary THA; allograft use during the first, second, third, or fourth revision arthroplasty; and analysis of the specimens at the time of death.

allograft cancellous chips, which were replaced by newly formed trabeculae⁷⁻⁹. Furthermore, the extent of allograft incorporation was found to be highly dependent on the particle size and processing of the bone graft⁵. Structural allografts were shown to support the acetabular architecture without being replaced by host bone, and with only minimal remodeling, in 2 cases¹⁰. Other studies of structural allografts in humans were limited to only clinical and radiographic results^{11,12}.

There have been many analyses of specimens retrieved from patients with failed THA. However, the incorporation of a successful implanted allograft at the site of a THA can be assessed only through long-term follow-up and subsequent micro-morphological analysis. In this study, we present what we believe to be the first comprehensive, multiscale analysis of structural allografts used in acetabular reconstruction. The study was conducted to analyze the quantitative and qualitative long-term integration properties of structural allografts in terms of the (1) allograft bone-host bone interface and structural properties of the allograft, (2) extent of allograft incorporation, and (3) mineralization properties.

Material and Methods

Specimen Recruitment

The names of all decedents with evidence of a THA were obtained from the largest local crematory and compared with a database that included all patients who had undergone revision THA combined with the use of structural allograft in the years 1987 to 2009. When there was a positive match, the cremation process was temporarily interrupted, and approval to obtain the

specimen for this study was obtained from the relatives. Key exclusion criteria were evidence of a systemic disorder affecting bone turnover (e.g., hyperparathyroidism or an inflammatory or renal disorder) and local changes within the pelvis (e.g., malignant tumor and Paget disease), which were determined by retrospective review of the medical records and by analysis of iliac crest biopsy specimens. The study was approved by the local ethics committee (WF-005/09) and complied with the Declaration of Helsinki. An overview of the recruitment procedure is shown in Figure 1.

Case Overview

Thirteen cases in which a structural allograft had been used for acetabular reconstruction were included in this study (Table I). Two additional cases were excluded because we were unable to identify sufficient allograft bone. The most common reason for THA revision was aseptic loosening of the acetabular cup with accompanying loss of bone from the superior dome or medial wall. None of the cases were affected by infectious or autoimmune joint disease. The mean interval from the primary THA (performed at a mean and standard deviation [SD] of 50.3 ± 9.9 years of age) to the acetabular reconstruction with implantation of a structural allograft (performed at a mean of 69.5 ± 7.9 years of age) was 19.2 years (Table II, Fig. 1). The mean duration for which the allograft was in situ was calculated as 12.9 ± 5.2 years (range, 4 to 22 years) on the basis of a mean age at death of 82.4 ± 7.8 years. All femoral allografts underwent thermal disinfection (at 101° to 109°C for 45 minutes) using a Lobator SD-2 system (Telos) and were subsequently cryopreserved at -80°C .

TABLE I Individual Patient Data

Case	Sex	Primary Disease	Secondary Diseases*	Operation at Which Bone Graft Used	Location of Bone Graft	Patient Age at Bone Graft (yr)	Duration of Bone Graft in Situ (yr)
1	F	Osteoarthritis	None	2nd revision (cup loosening)	Medial wall	67	14
2	M	Hip dysplasia, osteoarthritis	Hypertension, coronary artery disease, chronic venous insufficiency	1st revision (stem and cup loosening)	Medial wall, superior dome	66	15
3	F	Osteoarthritis	Hypertension, varicosis, hyperlipidemia	2nd revision (stem and cup loosening)	Medial wall, superior dome	73	22
4	F	Hip dysplasia, osteoarthritis	Parkinson disease	4th revision (recurrent dislocations and cup loosening)	Superior dome	66	7
5	M	Osteoarthritis	Not available	1st revision (stem fracture with cup loosening, material abrasion with chronic synovitis)	Medial wall, superior dome	50	15
6	F	Hip dysplasia, osteoarthritis	None	3rd revision (cup loosening with bone loss)	Superior dome	79	12
7	F	Femoral fracture	Hypertension, cardiac arrhythmia, GERD	2nd revision (stem and cup loosening)	Superior dome	61	19
8	F	Osteoarthritis	Ankylosing spondylitis, hypertension, hypothyroidism	2nd revision (cup loosening and cranial migration)	Superior dome	69	5
9	F	Hip dysplasia, osteoarthritis	None	2nd revision (recurrent cup loosening)	Superior dome	74	13
10	F	Osteoarthritis	Not available	2nd revision (osteonecrosis of acetabular roof)	Superior dome	67	17
11	M	Osteoarthritis	GERD, chronic obstructive pulmonary disease, coronary artery disease, hyperuricemia	1st revision (cup loosening with bone loss)	Superior dome, posterior column	79	9
12	F	Osteoarthritis	Hypertension, coronary artery disease, breast cancer	1st revision (stem and cup loosening)	Medial wall, superior dome	79	4
13	F	Not available	Hypertension, heart failure, obesity	1st revision (acetabular fracture with cup loosening)	Medial wall, superior dome	73	10

*GERD = gastroesophageal reflux disease.

Specimen Preparation

To determine the location and state of the allograft, contact radiographs of the pelvic explants were obtained shortly after death (Fig. 2-A). Previous clinical radiographs were evaluated in all cases as well. Furthermore, 3-dimensional imaging of the specimens was performed with high-resolution peripheral quantitative computed tomography (HR-pQCT; Scanco Medical) (Fig. 2-B). On the basis of the surgical reports and images obtained with the radiography and HR-pQCT, the location of the allograft within the acetabulum and the cut planes were determined. Two consecutive sections were cut using a diamond band saw (EXAKT). Additionally, transiliac iliac crest biopsies, as described by Bordier et al.¹³, were performed.

Preparation of Undecalcified Specimens, Grinding, and Histological Analysis

The obtained bone specimens were fixed in 3.7% formaldehyde, dehydrated in a graded series of ethanol solutions, and embedded in methylmethacrylate (Technovit 7200; EXAKT/Kulzer).

The cut sections of the acetabulum were ground to a thickness of approximately 30 μm and stained with toluidine blue. Additional 5- μm -thick sections were prepared from the acetabular

TABLE II Time Course of Relevant Procedures/Events and Location of Defects

Parameter	Mean \pm SD or No.
Age at primary THA (yr)	50.3 \pm 9.9
Time between primary THA and 1st revision (yr)	13.6 \pm 7.1
Age at bone graft (yr)	69.5 \pm 7.9
Duration of bone graft in situ (yr)	12.9 \pm 5.2
Age at death (yr)	82.4 \pm 7.8
Superior defect (no.)	6
Medial defect (no.)	1
Combined defect (no.)	6

sections and the iliac crest bone biopsy specimens and subsequently stained with toluidine blue, trichrome Masson-Goldner, and von Kossa/van Gieson stains. All sections were prepared in an undecalcified manner^{14,15}.

Analysis of Allograft: Host Bone Integration and Incorporation

Histological analysis was performed using an Olympus BX61 microscope equipped with a camera. The complete ground sections were scanned by merging 500 to 1,000 single images (50× magnification) to create a large image file covering an overall area of approximately 20 cm². The acquired high-resolution images formed the basis for the following evaluation with Olympus Stream Motion 2.1 imaging software.

The analysis of the incorporation properties required identification of the structural allograft bone, adjacent host bone, allograft bone-host bone interface, and original allograft bone border. Macroscopic images and contact radiographs of all sections were obtained (Figs. 2-C and 2-D). To analyze the current allograft bone-host bone interface, the allograft bone border (red line, Fig. 2-E), representing the most distant avital remnants from the allograft bone body, and the host bone border (blue line, Fig. 2-E), indicating the maximum ingrowth of the vital host bone penetrating the allograft bone, were determined. The mean distance between the host and allograft bone borders was determined by multiple, orthogonally orientated measurements (red lines, Fig. 2-E) and indicated the current overlap.

To analyze the total extent of osseoincorporation, the original allograft bone border (green line, Fig. 2-E) was identified on the basis of surgical reports on the location, dimensions, and shape of the femoral head allograft; radiographs; anatomical topography; and histomorphological changes in the bone microarchitecture. The distance to the host bone border (from the green line to the blue line, Fig. 2-E) was measured and indicated the total ingrowth. Calculation of the Cohen kappa coefficient (κ) revealed almost perfect interrater agreement ($\kappa > 0.90$) between the interface analyses of 2 of the investigators.

Quantitative Backscattered Electron Imaging

Quantitative backscattered electron imaging (qBEI) with a scanning electron microscope (LEO435VP; LEO Electron Microscopy) was used to assess the degree of mineralization in the center of the allograft bone and the host bone¹⁶⁻¹⁹. The generated mineralization profiles (gray value histogram) represent the mean Ca content, peak Ca content, and heterogeneity of mineralization (Ca width) of the cross-sectioned bone. The magnification used was 200× with an edge length of 1.135 μm for each pixel. Image thresholds were established with ImageJ software (National Institutes of Health) and used to evaluate the number of osteocyte lacunae per bone area (1/mm²) and the area of the osteocyte lacunae (μm^2).

Iliac Crest Histomorphometry

Histomorphometric analysis of the bone volume per tissue volume fraction, trabecular number, trabecular thickness, and

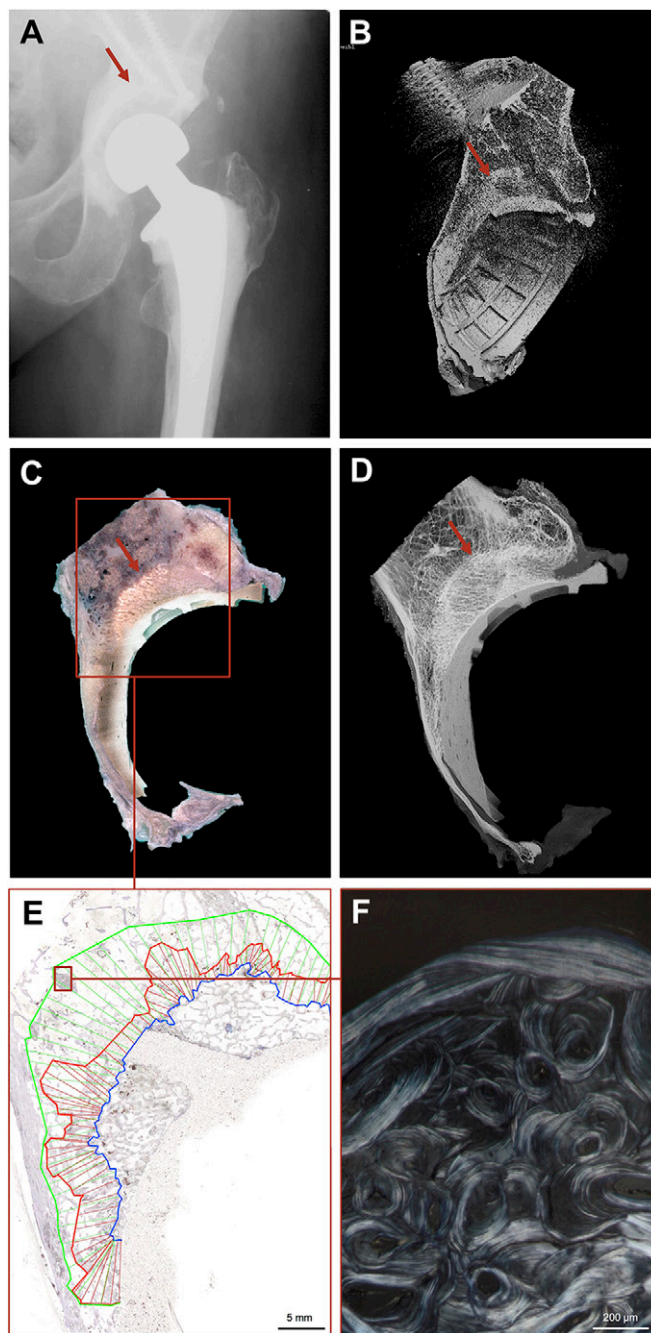


Fig. 2
Multiscale analysis of structural allograft incorporation. Red arrow = assumed location of the allograft. **Fig. 2-A** Anteroposterior radiograph made at the time of death. **Fig. 2-B** HR-pQCT scan indicates the 3-dimensional microstructural properties. **Fig. 2-C** Photograph of the cut section. **Fig. 2-D** Contact radiograph of the cut section. **Fig. 2-E** Microscopic overview of the ground section and determination of the interfaces. Blue line = host bone border, red line = allograft bone border, and green line = original allograft bone border. **Fig. 2-F** Polarized microscopy image indicating a cortical bone remnant from the allograft bone with an osteonal structure surrounded by cancellous vital host bone.

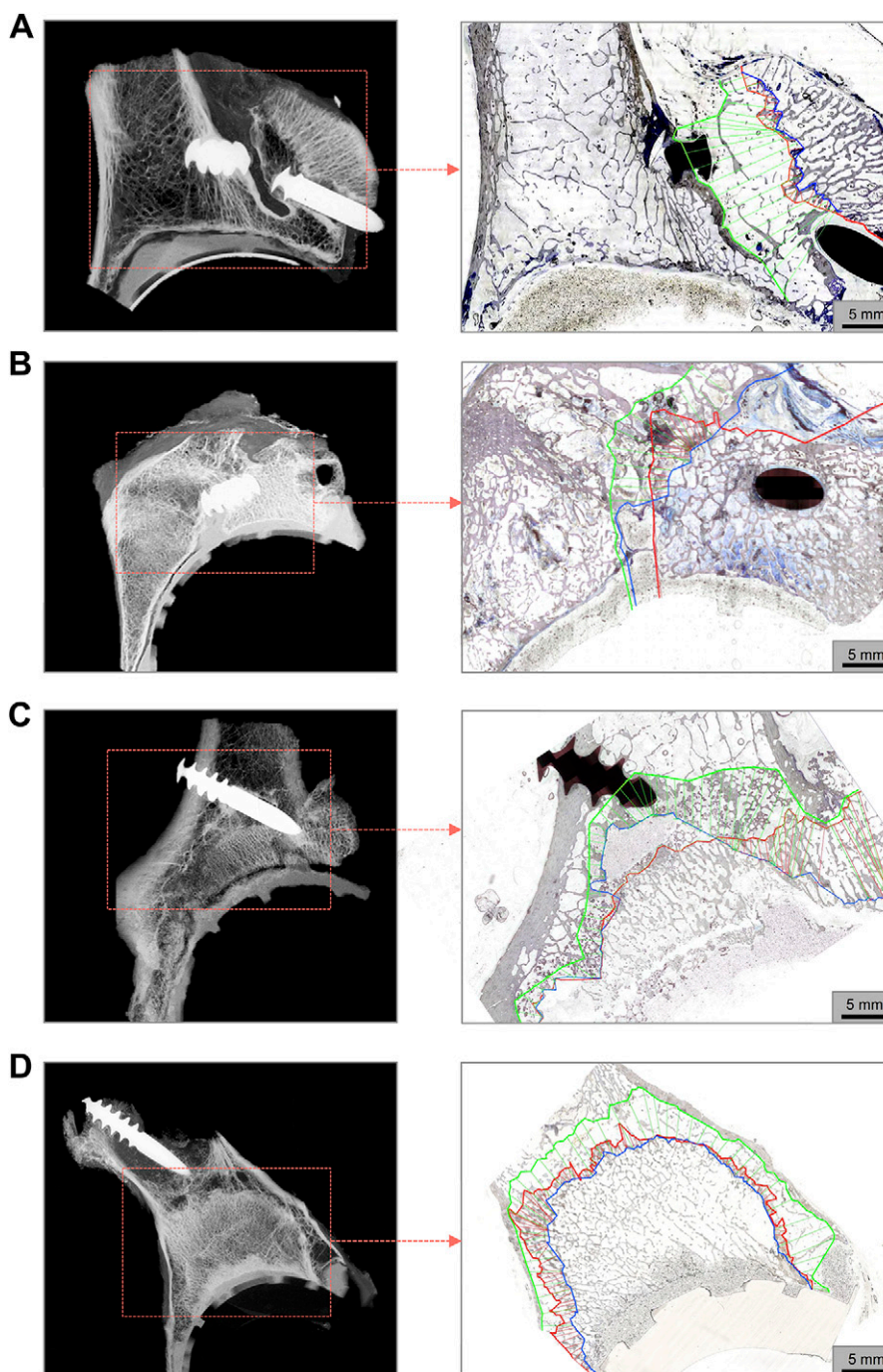


Fig. 3
Contact radiographs and the microscopic views of ground sections, showing successful osseoincorporation of structural allografts in Cases 4 (**Fig. 3-A**), 11 (**Fig. 3-B**), 2 (**Fig. 3-C**), and 8 (**Fig. 3-D**) (see Table I). The distance between the original allograft bone border (green line) and the host bone border (blue line) represents the total ingrowth, while the distance between the blue line and the red line (current allograft bone border) represents the current overlap.

trabecular separation was performed on histological sections of the iliac crest bone biopsy specimens to characterize the individual skeletal status at the time of death. The results were compared with those of age and sex-matched controls ($n = 110$) from our database²⁰.

Statistical Analysis

Results are presented as absolute values or means with the SD. To detect differences between the groups (host bone versus allograft bone and iliac crest microstructure in the study group versus that in the controls), the unpaired, 2-tailed Student t test

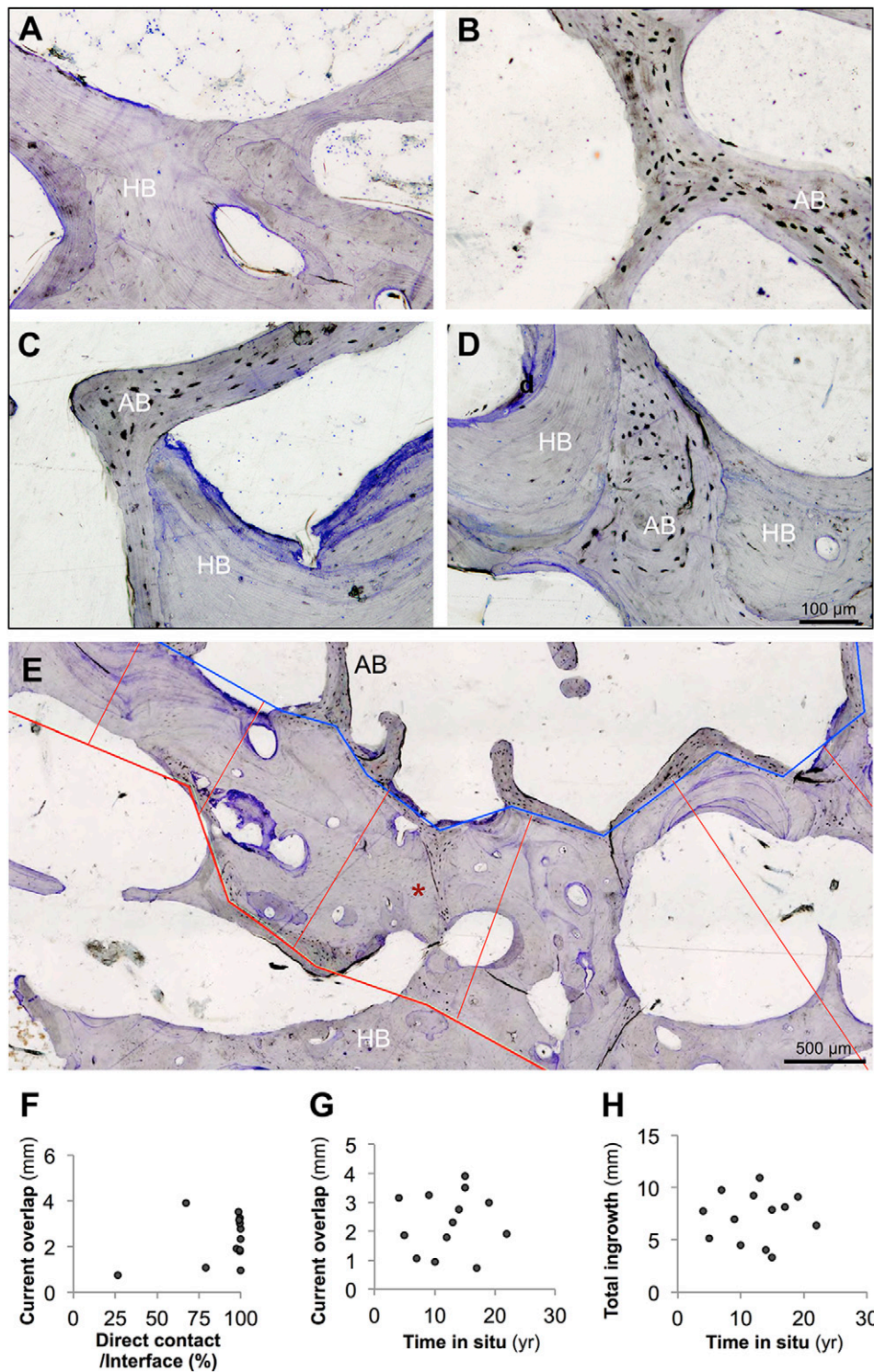


Fig. 4

Histological analysis of ingrowth parameters from toluidine-blue-stained ground sections. **Fig. 4-A** Vital host bone (HB) was identified by the presence of viable osteocytes within the bone matrix and vital bone marrow cells. **Fig. 4-B** Dead allograft bone (AB) demonstrated black (air-filled) osteocyte lacunae. **Figs. 4-C and 4-D** Successful remodeling of the allograft bone surrounded by the host bone. **Fig. 4-E** Analysis of the current allograft bone-host bone interface. Blue line = host bone border, red line = allograft bone border, and asterisk = current overlap area. **Figs. 4-F, 4-G, and 4-H** Regression analysis of the percentage of the interface with direct contact between the host and allograft bone and the current overlap (**Fig. 4-F**), the time in situ and the current overlap (**Fig. 4-G**), and the time in situ and total ingrowth (**Fig. 4-H**).

TABLE III Parameters of Ingrowth Between Host Bone and Allograft Bone

Parameter	Mean ± SD
Direct contact of host and allograft bone (% of interface)	89.6 ± 20.7
Current allograft bone-host bone overlap (% of interface)	78.6 ± 26.6
Mean current overlap (mm)	2.3 ± 1.0
Maximum current overlap (mm)	5.3 ± 2.4
Mean total ingrowth (mm)	7.2 ± 2.3
Maximum total ingrowth (mm)	10.5 ± 4.0

was used. The level of significance was defined as $p < 0.05$. Spearman rank correlation tests were performed to determine the relationship between the time that the allograft was in situ and the current overlap and the total ingrowth of the host bone as well as between the direct contact between the host and allograft bone and the current overlap.

Results

Characterization of Allograft and Host Bone

A dense body within the acetabulum surrounded by a sclerotic line was identified on the radiographs made of the pelvic explants, HR-pQCT scans, and contact radiographs of the cut sections (Figs. 2-A through 2-D). The macroscopic view of the sections cut through the center of the structural allograft showed a bright body while the surrounding cancellous bone presented with a typical brown and red color as a sign of vital, vascularized bone marrow (Fig. 2-C). A second sclerotic line, indicating the original allograft bone border, was found in most cases. Remnants of the cortical bone from the transplanted femoral head within the vital cancellous acetabular bone could be determined and were confirmed by polarized microscopy showing the osteonal structure (Figs. 2-D, 2-E, and 2-F).

The presence of allograft bone was confirmed by the histological evaluation in all 13 cases (Figs. 2-E and 3). We observed a uniform, recurrent histological pattern, with the host bone identified mostly by viable osteocytes within the trabeculae and by vital bone marrow with fat cells (Fig. 4-A). In contrast, the allograft bone body consisted of thick, well-structured trabeculae (see Appendix) with empty osteocyte lacunae (black appearance) and necrotic soft tissue. There were no vital cells or signs of revascularization (Fig. 4-B). The peripheral area of the allograft was penetrated by newly formed vital bone, which was deposited on the avital trabeculae, and the necrotic tissue was replaced by fibrosis (Figs. 4-C and 4-D).

Multiscale Analysis of Bone Allograft Incorporation

The region of overlapping host and allograft bone was enclosed by the host bone border (blue line) and the allograft bone border (red line) (Fig. 4-E). In 10 of the 13 cases, 100% of the interface was characterized by direct contact and

additional overlap of the allograft bone and host bone, while the remaining 3 cases demonstrated direct contact along 25% to 80% of the interface. On average, there was direct allograft bone-host bone contact along 89.6% of the interface and overlap of the allograft bone and host bone along 78.6% of the interface, indicating an overall tight junction of the allograft and host bone.

The current overlap averaged 2.3 ± 1.0 mm, with a maximum of 5.3 ± 2.4 mm (Table III). The total ingrowth reached much further, averaging 7.2 ± 2.3 mm with a maximum of 10.5 ± 4.0 mm (Fig. 3, Table III). Further analysis revealed no significant correlations between the current overlap or total ingrowth and the time that the allograft had been in situ or between the current overlap and the percentage of the interface with direct allograft bone-host bone contact (Figs. 4-F, 4-G, and 4-H). Where there was no direct contact or overlap of the host and allograft bone, these 2 components were separated by fibrous tissues and no signs of remodeling were detectable. Furthermore, mechanical barriers, such as screws and tantalum wedges, resulted in the absence of local remodeling with insufficient incorporation of the graft around these barriers.

Mineralization and Osteocyte Analysis

The mean and peak calcium concentrations assessed with qBEI were significantly higher in the allograft bone center than in the host bone (Figs. 5-A, 5-B, and 5-C). The SD of the calcium distribution, indicating the mineralization heterogeneity, did not differ between groups (calcium width, Fig. 5-D). Overall, the bone mineral density distribution was altered in the allograft bone, indicating low or no bone remodeling (Fig. 5-E). The number of osteocyte lacunae and the lacunar area were significantly lower in the allograft bone, indicating an avital bone matrix (Figs. 5-F and 5-G). Furthermore, a high number of hypermineralized, micropetrotic lacunae was seen in the allograft bone (Fig. 5-A, red arrows).

Compromised Overall Bone Status in Iliac Biopsy Specimens

A histomorphometric analysis of the iliac crest bone biopsy specimens revealed a highly diminished overall bone status expressed by a significantly decreased bone volume per tissue volume fraction ($7.0\% \pm 3.0\%$) compared with that of the age and sex-matched control cohort²⁰ ($12.7\% \pm 5.7\%$; $p < 0.001$). No significant difference in trabecular number, thickness, or separation was detected between the study and control groups because of a high SD in the control group (Table IV).

Discussion

In this study, we demonstrated that structural allografts used for acetabular reconstruction undergo incorporation and subsequent remodeling. It is remarkable that the incorporation was observed at the allograft bone-host bone interface in all cases, especially because a previous study of 2 structural allografts showed only minor evidence of bone union¹⁰. These contrasting observations can be explained by the fact that, in the previous study, there was little direct contact between the host and allograft bone, while close contact of the host and

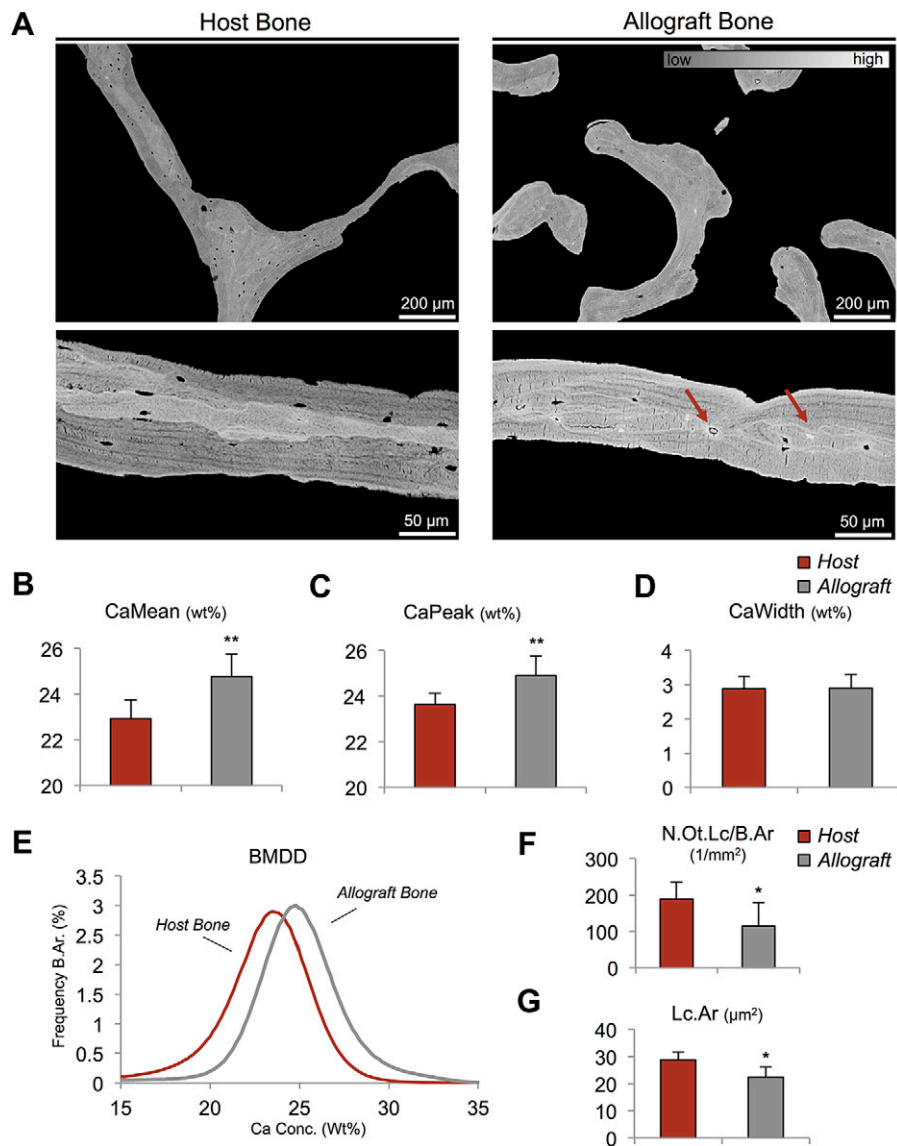


Fig. 5

Results of qBEI analysis. The error bars on the graphs indicate the standard deviation (SD). **Fig. 5-A** Allograft bone revealed higher mineralization than the host bone, as expressed by the differences in the gray values. Red arrows = hypermineralized (micropetrotic) osteocyte lacunae in allograft bone. **Fig. 5-B** Mean calcium content. $**P < 0.001$. **Fig. 5-C** Calcium peak values, indicating the most frequent calcium content. $**P < 0.001$. **Fig. 5-D** Calcium width, indicating the mineralization heterogeneity. **Fig. 5-E** Overall bone mineral density distribution (BMDD), indicating a higher matrix mineralization in allograft bone. B.Ar = bone area. **Fig. 5-F** The number of osteocyte lacunae per bone area (N.Ot.Lc/B.Ar). $*P < 0.05$. **Fig. 5-G** Lacunar area (Lc.Ar). $*P < 0.05$.

allograft bone was obtained in the cases in the present study. However, a time-dependent progression of ingrowth was not found. In fact, the center of the allograft bone remained unchanged and partly encapsulated by fibrous tissue even in the case in which the allograft had been in situ for the most time. Union at cortical-cortical junctions but no remodeling of the allograft has been observed in allografts used in tumor reconstructions²¹. With cortical interfaces being fundamentally different from trabecular structures, a time-dependent increase of incorporation was also not found; however, it has to be noted

that most of the patients included in that study had received chemotherapy²¹.

A tight junction is most likely a prerequisite for a successful remodeling process and consecutive incorporation of the allograft bone. Remodeling of the allograft bone was absent in sections with barriers, such as screws and cement, with a fibrous tissue gap between the host and allograft bone. Furthermore, direct contact with only a minimum of micromovement was essentially reported to be mandatory for osseointegration of prosthetic components². However, it is also possible that small gaps between the host and

TABLE IV Bone Histomorphometry Results in Iliac Crest Compared with Reference (Control) Values²⁰

Parameter	Mean ± SD		P Value
	Cases 1-13	Controls (N = 110)	
Bone volume/ tissue volume (%)	7.0 ± 3.0	12.7 ± 5.7	<0.001
Trabecular number (1/mm)	0.7 ± 0.2	0.9 ± 0.4	>0.05*
Trabecular thickness (μm)	105.4 ± 33.1	154.9 ± 118.2	>0.05*
Trabecular separation (μm)	1,521.9 ± 565.8	1,257.2 ± 685.4	>0.05*

*Not significant.

allograft bone were bridged given the presence of 2 potentially osteoconductive surfaces.

Direct contact and bone remodeling were achieved in the majority of the interfaces in our cases, and all had incorporation of the allograft bone. However, the allograft bone center remained acellular, which is in accordance with previous findings²². We previously found that synthetic bone materials (beta-tricalcium-phosphate bone substitutes) are also not completely remodeled and incorporated over time, although the clinical outcomes were good²³.

Histological analysis of cancellous chip grafts used in humans revealed a completely incorporated, newly formed bone structure⁷. This structure was observed to a large extent in the structural allografts examined in our study, with maximum ingrowth limited to a mean of 10.5 mm. The difference in incorporation between the chips and structural allografts may be at least partially explained by the different surgical techniques and processing of the allograft bone. While the original structure of the allograft bone is maintained in structural allografts²⁴, impaction grafting ensures a tight junction of the cancellous chips with the host bone²⁵. Furthermore, morselized or particulate bone may be more accessible to the bone cells (i.e., osteoblasts and osteoclasts) because of its larger surface and may therefore have improved osteoconductive capacities^{5,26,27}.


Another influential factor is that structural allografts are commonly used in patients with severe bone loss and an overall compromised bone status, as confirmed by the iliac crest histomorphometry in this study. In such cases, the reduced bone mass might be the result of a general imbalance in bone remodeling (e.g., low bone formation), which has possible negative effects on the incorporation. In general, many factors (e.g., age and weight-bearing) may influence the extent of allograft bone incorporation, which could be the reason for the absence of a time-dependent increase in the ingrowth found in this study. Furthermore, a large proportion of the incorporation process may be completed within the first weeks, while afterward a steady state is achieved. This was also seen in an experimental study of cancellous chips in a goat model, in which the largest part of the graft had become incorporated within 12 weeks⁹.

The results of electron microscopy confirmed that the center of the allograft bone was not subject to remodeling, as the allograft bone matrix was highly mineralized with a low number of small osteocyte lacunae. The accumulation of micropetrotic lacunae, which were previously described in aged bone¹⁸, explains this finding. Furthermore, it is not clear whether micropetrosis represents an active or passive mechanism within the bone²⁸; the findings in this study suggest that it represents a passive mechanism.

A limitation of the study was that 2-dimensional sections provide only limited insight into the 3-dimensional process of bone remodeling. However, this study not only included a large number of cases with long-term follow-up but also was based on the analysis of complete pelvic explants, in contrast to studies of biopsy specimens only, and therefore conclusively clarifies the extent of incorporation of structural allografts in acetabular reconstruction.

In conclusion, we found clear evidence of osseoincorporation and revitalization of the allograft in all cases with tight contact between the host and graft bone. The remaining unremodeled allograft structures were adequately mineralized and showed no signs of collapse up to 22 years after transplantation, suggesting a substantial contribution to continuous acetabular stability and thus indicating clinical success.

Appendix

 A table showing microstructural parameters within the allografts is available with the online version of this article as a data supplement at [jbjs.org \(http://links.lww.com/JBJS/E855\)](http://links.lww.com/JBJS/E855). ■

Note: The authors thank E. Leicht and M. Dietzmann for technical assistance in preparing the histological sections as well as Prof. Matthias Gebauer and Dr. Marius Arndt for their help with the clinical data, Dr. Björn Busse and Christoph Riedel for their support and assistance with the backscattered electron imaging, and Dr. Christian Friecke for his support in the early phase of the study.

Sebastian Butscheidt, MD¹
Menard Moritz, MD¹
Thorsten Gehrke, MD²
Klaus Püschel, MD¹
Michael Amling, MD¹
Michael Hahn, PhD¹
Tim Rolvien, MD¹

¹Departments of Osteology and Biomechanics (S.B., M.M., M.A., M.H., and T.R.), Legal Medicine (K.P.), and Orthopaedic Surgery (T.R.), University Medical Center Hamburg-Eppendorf, Hamburg, Germany

²Helios Endo Clinic Hamburg, Hamburg, Germany

E-mail address for M. Amling: amling@uke.de

ORCID iD for S. Butscheidt: [0000-0002-1849-5000](https://orcid.org/0000-0002-1849-5000)

ORCID iD for M. Moritz: [0000-0002-3164-3717](https://orcid.org/0000-0002-3164-3717)

ORCID iD for T. Gehrke: [0000-0002-4124-1682](https://orcid.org/0000-0002-4124-1682)

ORCID iD for K. Püschel: [0000-0002-1362-1311](https://orcid.org/0000-0002-1362-1311)

ORCID iD for M. Amling: [0000-0003-2382-8348](https://orcid.org/0000-0003-2382-8348)

ORCID iD for M. Hahn: [0000-0002-7400-5571](https://orcid.org/0000-0002-7400-5571)

ORCID iD for T. Rolvien: [0000-0003-1058-1307](https://orcid.org/0000-0003-1058-1307)

References

1. Bozic KJ, Kurtz SM, Lau E, Ong K, Vail TP, Berry DJ. The epidemiology of revision total hip arthroplasty in the United States. *J Bone Joint Surg Am.* 2009 Jan;91(1):128-33.
2. Pilliar RM, Lee JM, Maniopoulos C. Observations on the effect of movement on bone ingrowth into porous-surfaced implants. *Clin Orthop Relat Res.* 1986 Jul;208:108-13.
3. Deirmengian GK, Zmistowski B, O'Neil JT, Hozack WJ. Management of acetabular bone loss in revision total hip arthroplasty. *J Bone Joint Surg Am.* 2011 Oct 5;93(19):1842-52.
4. Jasty M, Harris WH. Salvage total hip reconstruction in patients with major acetabular bone deficiency using structural femoral head allografts. *J Bone Joint Surg Br.* 1990 Jan;72(1):63-7.
5. Malinin TI, Carpenter EM, Temple HT. Particulate bone allograft incorporation in regeneration of osseous defects; importance of particle sizes. *Open Orthop J.* 2007 Dec 18;1:19-24.
6. Fox R. New bone? *Lancet.* 1992 Feb 22;339(8791):463-4.
7. van der Donk S, Buma P, Slooff TJ, Gardeniers JW, Schreurs BW. Incorporation of morselized bone grafts: a study of 24 acetabular biopsy specimens. *Clin Orthop Relat Res.* 2002 Mar;396:131-41.
8. Schreurs BW, Buma P, Huiskes R, Slagter JL, Slooff TJ. Morsellized allografts for fixation of the hip prosthesis femoral component. A mechanical and histological study in the goat. *Acta Orthop Scand.* 1994 Jun;65(3):267-75.
9. Schimmel JW, Buma P, Versleyen D, Huiskes R, Slooff TJ. Acetabular reconstruction with impacted morselized cancellous allografts in cemented hip arthroplasty: a histological and biomechanical study on the goat. *J Arthroplasty.* 1998 Jun;13(4):438-48.
10. Hooten JP Jr, Engh CA, Heekin RD, Vinh TN. Structural bulk allografts in acetabular reconstruction. Analysis of two grafts retrieved at post-mortem. *J Bone Joint Surg Br.* 1996 Mar;78(2):270-5.
11. Garbuz D, Morsi E, Gross AE. Revision of the acetabular component of a total hip arthroplasty with a massive structural allograft. Study with a minimum five-year follow-up. *J Bone Joint Surg Am.* 1996 May;78(5):693-7.
12. Shinar AA, Harris WH. Bulk structural autogenous grafts and allografts for reconstruction of the acetabulum in total hip arthroplasty. Sixteen-year-average follow-up. *J Bone Joint Surg Am.* 1997 Feb;79(2):159-68.
13. Bordier P, Matrajt H, Miravet L, Hioco D. [Histological measure of the volume and resorption of bone joints]. *Pathol Biol.* 1964 Dec;12:1238-43. French.
14. Donath K. Die Trenn-Dünnschliff-Technik zur herstellung histologischer präparate von nicht schneidbaren gewebe und materialien. *Der Präparator.* 1988;34:197-206.
15. Hahn M, Vogel M, Delling G. Undecalcified preparation of bone tissue: report of technical experience and development of new methods. *Virchows Arch A Pathol Anat Histopathol.* 1991;418(1):1-7.
16. Koehne T, Vettorazzi E, Küsters N, Lüneburg R, Kahl-Nieke B, Püschel K, Amling M, Busse B. Trends in trabecular architecture and bone mineral density distribution in 152 individuals aged 30-90 years. *Bone.* 2014 Sep;66:31-8. Epub 2014 May 23.
17. Roschger P, Paschalis EP, Fratzi P, Klaushofer K. Bone mineralization density distribution in health and disease. *Bone.* 2008 Mar;42(3):456-66. Epub 2007 Nov 12.
18. Busse B, Djonic D, Milovanovic P, Hahn M, Püschel K, Ritchie RO, Djuric M, Amling M. Decrease in the osteocyte lacunar density accompanied by hyper-mineralized lacunar occlusion reveals failure and delay of remodeling in aged human bone. *Aging Cell.* 2010 Dec;9(6):1065-75. Epub 2010 Oct 28.
19. Rolvien T, Krause M, Jeschke A, Yorgan T, Püschel K, Schinke T, Busse B, Demay MB, Amling M. Vitamin D regulates osteocyte survival and perilacunar remodeling in human and murine bone. *Bone.* 2017 Oct;103:78-87. Epub 2017 Jun 27.
20. Priemel M, von Domarus C, Klatte TO, Kessler S, Schlie J, Meier S, Proksch N, Pastor F, Netter C, Streichert T, Püschel K, Amling M. Bone mineralization defects and vitamin D deficiency: histomorphometric analysis of iliac crest bone biopsies and circulating 25-hydroxyvitamin D in 675 patients. *J Bone Miner Res.* 2010 Feb;25(2):305-12.
21. Enneking WF, Campanacci DA. Retrieved human allografts: a clinicopathological study. *J Bone Joint Surg Am.* 2001 Jul;83(7):971-86.
22. Hooten JP Jr, Engh CA Jr, Engh CA. Failure of structural acetabular allografts in cementless revision hip arthroplasty. *J Bone Joint Surg Br.* 1994 May;76(3):419-22.
23. Rolvien T, Barvencik F, Klatte TO, Busse B, Hahn M, Rueger JM, Rupprecht M. 8-TCP bone substitutes in tibial plateau depression fractures. *Knee.* 2017 Oct;24(5):1138-45. Epub 2017 Jul 13.
24. Inoue D, Kabata T, Maeda T, Kajino Y, Yamamoto T, Takagi T, Omori T, Tsuchiya H. The value of bulk femoral head allograft in acetabular reconstruction using Kerboul-type plate. *Int Orthop.* 2015 Sep;39(9):1839-44. Epub 2015 Jul 12.
25. Delloye C, Cornu O, Druetz V, Barbier O. Bone allografts: what they can offer and what they cannot. *J Bone Joint Surg Br.* 2007 May;89(5):574-9.
26. Aspenberg P, Tägil M, Kristensson C, Lidin S. Bone graft proteins influence osteoconduction. A titanium chamber study in rats. *Acta Orthop Scand.* 1996 Aug;67(4):377-82.
27. Thorén K, Aspenberg P, Thorgren KG. Lipid extracted bank bone. Bone conductive and mechanical properties. *Clin Orthop Relat Res.* 1995 Feb;311:232-46.
28. Milovanovic P, Zimmermann EA, Vom Scheidt A, Hoffmann B, Sarau G, Yorgan T, Schweizer M, Amling M, Christiansen S, Busse B. The formation of calcified nanospherites during micropetrosis represents a unique mineralization mechanism in aged human bone. *Small.* 2017 Jan;13(3). Epub 2016 Nov 7.